Circulant matrix-based Box-Behnken designs with economic run sizes

Tung-Dinh Pham[*], Nam-Ky Nguyen[†]

May 24, 2026

Abstract

We introduce *Circulant Matrix-Based Box–Behnken Designs* (CBBDs), a new class of three-level, second-order response surface designs constructed using circulant matrix structures. These designs satisfy an *enhanced orthogonal minimally aliased* (OMA*) property: they retain the classical OMA property—where main effects are orthogonal to each other and to all second-order effects (i.e., quadratic effects and two-factor interaction effects) -and further ensure orthogonality between quadratic and interaction effects. An efficient algorithm is developed for generating CBBDs, and a catalog of designs for up to 11 factors is provided. The resulting designs exhibit high D-efficiency, support full estimation of second-order models, and preserve most of the desirable features of traditional Box–Behnken Designs, while requiring fewer experimental runs. These properties make CBBDs a practical and resource-efficient alternative for complex experimental settings.

AMS Classification: 62K20

Keywords: *D*-efficiency; Circulant matrices; Orthogonal minimally aliased response surface designs; OMARS designs; Response surface designs.

Funding: No funding was received.

[*]VNU University of Science, Vietnam National University, Hanoi, Vietnam; email: tungpd@vnu.edu.vn

[†]Vietnam Institute for Advanced Study in Mathematics, Hanoi, Vietnam; email: nknam@viasm.edu.vn

1 Introduction

Box–Behnken Designs (BBDs), introduced by Box and Behnken (1960), are three-level response surface designs widely used in response surface methodology (RSM) to efficiently estimate second-order models. BBDs are constructed from balanced incomplete block designs (BIBDs) or partially BIBDs (Nguyen and Borkowski, 2008) and strategically combine high, low, and center levels for each factor. This structure offers substantial run-size savings compared with full factorial or central composite designs, enabling efficient estimation of full second-order models while conserving experimental resources. All BBDs are spherical designs, meaning each run contains the same number of nonzero (± 1) factor settings, resulting in design points located on or near a hypersphere in factor space. A key statistical advantage of BBDs is that they satisfy what is commonly referred to as the orthogonal minimally aliased (OMA) property (Núñez Ares and Goos, 2020), under which main effects (MEs) are orthogonal to one another and to all second-order effects, i.e. quadratic effects (QEs) and two-factor interaction effects (IEs). In fact, traditional BBDs possess a stronger structure: QEs and IEs are also mutually orthogonal. In this paper, we distinguish between the classical OMA definition—requiring orthogonality between MEs and second-order effects—and an enhanced OMA, OMA* property, which additionally requires orthogonality between QEs and IEs. Under this terminology, BBDs satisfy the OMA* property. This orthogonal structure reduces confounding and simplifies interpretation, making BBDs a standard choice in industrial and scientific experimentation.

Despite these advantages, BBDs grow rapidly in size as the number of factors increases. For example, BBDs for five, six, and seven factors require 40, 48, and 56 runs respectively (excluding center points), while an eight-factor BBD requires at least 120 runs and a 12-factor version nearly 200 runs. Moreover, factor columns in BBDs are sparse, often containing more than 50% zeros, which restricts coverage of extreme factor combinations and can limit the detection of higher-order or complex response surface features.

A motivating example is provided by Gan, Fang, and Wei (2021), who studied how landing gear strut friction affects touchdown performance in light aircraft. Their experiment sought to optimize parameters for improved energy absorption and impact response using a validated numerical model of a half-axle landing gear system with an oleo-pneumatic shock absorber. An eight-factor BBD was employed, including: (i) strut geometric length, (ii) strut outer diameter, (iii) bearing width, (iv) piston rod diameter, (v) wheel inertia, (vi) strut installation angle, (vii) strut offset distance, and (viii) area moment of inertia of structural components. This design required 112 non-center runs located at the midpoints of edges in the factor space, plus eight center runs, for a total of 120 runs. Each factor column contained 28 nonzero values ± 1's and 84 0's, illustrating the sparse structure typical of BBDs. While such designs are statistically robust, their large run size and high proportion of zeros highlight limitations in design economy and geometric flexibility.

To address these challenges, this paper introduces *Circulant Matrix-Based Box–Behnken Designs* (CBBDs), a new class of three-level, second-order response surface designs constructed using circulant matrix structures. The proposed designs preserve the same orthogonality structure as traditional BBDs—namely, the OMA* property —while substantially reducing the required number of runs and improving geometric coverage. Like BBDs, CBBDs are spherical, with equal numbers of nonzero entries in each run. An efficient algorithm for constructing CBBDs is developed, and a catalog of designs for up to 11 factors is provided. These designs exhibit high D-efficiency, support full estimation of second-order models, and retain the key statistical advantages of classical BBDs, making them a practical and resource-efficient alternative for complex experimental settings.

2 The Structure of CBBDs

Let $\mathbf{D} = (x_{ij})$ denote an $n \times m$ design matrix for a three-level experiment. The full second-order model for m factors in n runs is

$$y_u = \beta_0 + \sum_{i=1}^{m} \beta_i x_{ui} + \sum_{i=1}^{m} \beta_{ii} x_{ui}^2 + \sum_{i<j} \beta_{ij} x_{ui} x_{uj} + \epsilon_u, \tag{1}$$

where ϵ_u is the random error for observation y_u. The coefficients β_0, β_i, β_{ii}, and β_{ij} represent the intercept, MEs, QEs, and IEs, respectively.

A three-level design has the OMA property if the MEs are orthogonal to one another and to all SOEs (QEs and IEs). More details on the OMA property can be found in Jones and Nachtsheim (2011), Georgiou, Stylianou and Aggarwal (2014), Núñez Ares and Goos (2020), Nguyen et al. (2026). We extend this concept by defining the OMA* (enhanced OMA) property, which additionally requires orthogonality between QEs and IEs. A design satisfies the OMA* property if conditions (2a)–(2e) below hold:

$$\sum_{u=1}^{n} x_{ui} = 0 \qquad \forall\ i, \tag{2a}$$

$$\sum_{u=1}^{n} x_{ui} x_{uj} = 0 \qquad \forall\ i < j, \tag{2b}$$

$$\sum_{u=1}^{n} x_{ui} x_{uj}^2 = 0 \qquad \forall\ i < j, \tag{2c}$$

$$\sum_{u=1}^{n} x_{ui} x_{uj} x_{uk} = 0 \qquad \forall\ i < j < k, \tag{2d}$$

$$\sum_{u=1}^{n} x_{ui}^2 x_{uj} x_{uk} = 0 \qquad \forall\ i < j < k. \tag{2e}$$

We construct CBBDs by vertically concatenating r right-circulant matrices:

$$\mathbf{D} = \begin{pmatrix} \mathbf{C}^{(1)} \\ \vdots \\ \mathbf{C}^{(r)} \end{pmatrix}, \tag{3}$$

where each $\mathbf{C}^{(s)}$ is generated from a seed vector $\mathbf{c}^{(s)} = (c_0^{(s)}, \ldots, c_{m-1}^{(s)})'$. The (i,j)-th entry of $\mathbf{C}^{(s)}$ is $c^{(s)}_{(j-i) \bmod m}$, $i, j = 0, \ldots, m-1$, so that each subsequent row is obtained by a cyclic right shift of the previous row, yielding the standard right-circulant structure

$$\begin{pmatrix} c_0 & c_1 & \cdots & c_{m-1} \\ c_{m-1} & c_0 & \cdots & c_{m-2} \\ \vdots & \vdots & \ddots & \vdots \\ c_1 & c_2 & \cdots & c_0 \end{pmatrix}. \tag{4}$$

For $\mathbf{D}$ to satisfy the OMA* conditions (2a)–(2e), it suffices that the generating vectors $\mathbf{c}^{(s)}$ satisfy:

$$\sum_{s=1}^{r} \sum_{i=0}^{m-1} c_i^{(s)} = 0, \tag{5a}$$

$$\sum_{s=1}^{r} \sum_{i=0}^{m-1} c_i^{(s)} \, c^{(s)}_{(j-i) \bmod m} = 0, \qquad \forall\ j = 1, \ldots, m-1, \tag{5b}$$

$$\sum_{s=1}^{r} \sum_{i=0}^{m-1} c_i^{(s)} \left(c^{(s)}_{(j-i) \bmod m}\right)^2 = 0, \qquad \forall\ j = 1, \ldots, m-1, \tag{5c}$$

$$\sum_{s=1}^{r} \sum_{i=0}^{m-1} c_i^{(s)} \, c^{(s)}_{(j-i) \bmod m} \, c^{(s)}_{(k-i) \bmod m} = 0, \qquad \forall\ 1 \le j < k \le m-1, \tag{5d}$$

$$\sum_{s=1}^{r} \sum_{i=0}^{m-1} (c_i^{(s)})^2 \, c^{(s)}_{(j-i) \bmod m} \, c^{(s)}_{(k-i) \bmod m} = 0, \qquad \forall\ 1 \le j < k \le m-1. \tag{5e}$$

Remarks

1. Verifying conditions (5a)–(5e) is computationally more efficient than checking (2a)–(2e), since only r seed vectors of length m need to be examined, rather than the full $rm \times m$ design matrix. Moreover, condition (5a) is automatically satisfied if the total numbers of $+1$ and -1 entries across all seed vectors are balanced.

2. A design is called *foldover* if its runs can be partitioned into two equal halves such that the second half is obtained by row-wise sign reversal of the first. A design is *non-foldover* if it does not admit such a partition. If $\mathbf{D}$ is a foldover CBBD whose half-design fraction (HDF) satisfies condition (5b), then $\mathbf{D}$ has the OMA property. If, in addition, condition (5e) holds, then $\mathbf{D}$ satisfies the OMA* property.

Figure 1(a) presents a non-foldover CBBD for five factors with 40 runs (excluding center runs). The design consists of eight circulant matrices of order five, generated by the following eight seed vectors: `(--0--;+-0+-;+0+--;+0+++;-0++-;+-0-+;-++0-;+-+0-)`, where the symbols + and − represent $+1$ and -1, respectively.

(a)

```
--0--    +-0+-    +0+--    +0+++    -0++-    +-0-+    -++0-    +-+0-
---0-    -+-0+    -+0+-    ++0++    --0++    ++-0-    --++0    -+-+0
----0    +-+-0    --+0+    +++0+    +--0+    -++-0    0--++    0-+-+
0----    0+-+-    +--+0    ++++0    ++--0    0-++-    +0--+    +0-+-
-0---    -0+-+    0+--+    0++++    0++--    -0-++    ++0--    -+0-+
```

(b)

```
0----    0--++    +-0-+    0+-+-    0++++    0++--    -+0+-    0-+-+
-0---    +0--+    ++-0-    -0+-+    +0+++    -0++-    --+0+    +0-+-
--0--    ++0--    -++-0    +-0+-    ++0++    --0++    +--+0    -+0-+
---0-    -++0-    0-++-    -+-0+    +++0+    +--0+    0+--+    +-+0-
----0    --++0    -0-++    +-+-0    ++++0    ++--0    +0+--    -+-+0
```

Figure 1: Two CBBDs for $(m, r, n_1) = (5, 8, 4)$: (a) with a non-foldover structure; (b) with a foldover structure.

Figure 1(b) presents a foldover CBBD for five factors with 40 runs (excluding center runs). The design consists of eight circulant matrices of order five, but only four distinct

seed vectors are required. The first half-design fraction (HDF) is generated from the seed vectors `(0----;0--++;+-0-+;0+-+-)`. The second HDF is obtained by row-wise sign reversal of the first HDF.

3 The CBBD Algorithm

The CBBD algorithm constructs circulant matrix–based designs by optimizing the generating vectors of circulant matrices to satisfy the OMA* conditions. The algorithm performs a local search that iteratively modifies the generating vectors to minimize a penalty function measuring violations of these conditions.

Let C be an $r \times m$ matrix where r is the number of generating vectors of circulant matrices and m is the number of factors. Each row of C generates an $m \times m$ circulant block, producing a design with $n = rm + n_0$ runs, where n_0 denotes the number of center runs (typically $n_0 = 2$).

To monitor violations of the OMA* conditions (5a)–(5e), the algorithm constructs a vector J of length l. Each element of J corresponds to a moment condition derived from the generating vectors. Note that condition (5a) is automatically satisfied in the non-foldover case by imposing a zero sum on all entries of C, and it holds trivially in the foldover case. Hence, the length of J is

$$l = \begin{cases} 2(m-1) + (m-1)(m-2), & \text{for non-foldover designs,} \\ (m-1) + (m-1)(m-2)/2, & \text{for foldover designs.} \end{cases} \tag{6}$$

The penalty function is defined as $S = \sum_{j=1}^{l} J_j^2$, which measures the total violation of the OMA* conditions. A design satisfying all OMA* conditions corresponds to $S = 0$. Examples of the use of vector J in constructing three-level designs can be found in Pham et al. (2020). The algorithm proceeds as follows:

(i) **Step 1: Initialization.** Construct a matrix C of size $r \times m$. Each row contains n_1 nonzero entries (± 1) and $(m - n_1)$ zeros, subject to the constraint that the sum of all nonzero elements of C equals zero. The positions of these entries are randomized within each row. The vector J is then computed by accumulating the contributions of all rows of C according to the OMA* conditions (5a)–(5e). The current penalty value is computed as $S = \sum J_j^2$.

(ii) **Step 2: Iterative Optimization.** The algorithm searches for improvements by examining pairs of entries in C. Let (u, k) and (v, l) denote two positions in C. A swap is considered only if ($u = v$ and $C_{uk} \neq C_{ul}$) or ($u \neq v$ and $C_{uk} = -C_{vl}$). For each admissible pair, the algorithm evaluates the penalty value that would result from performing the swap. The swap producing the largest reduction in S is selected. If such a swap exists, it is executed and the vector J is updated accordingly. This procedure is repeated until either $S = 0$ or no further reduction in S is possible.

(iii) Step 3: Design Evaluation and Selection. When a configuration with $S = 0$ is obtained, the corresponding design matrix $\mathbf{D}$ is constructed from the circulant blocks generated by C. Let r_{QQ} and r_{II} denote the maximum absolute correlations among the quadratic effects (QEs) and interaction effects (IEs), respectively. If $\max(r_{QQ}, r_{II}) < c$, where c is a prespecified threshold controlling these correlations (e.g., 0.5 or 0.6), the D-efficiencies are computed as

$$d = \frac{1}{n} |\mathbf{X}'\mathbf{X}|^{1/p}, \tag{7}$$

where $\mathbf{X}$ is the model matrix of $\mathbf{D}$ and p is the number of parameters in the model. In this paper, d_1 and d_2 denote the D-efficiencies for the models including the intercept plus main effects (MEs), and the intercept plus MEs, QEs, and IEs, respectively. Each candidate design is then evaluated using the vector $f = (1 - d_2,\ r_{II},\ r_{QQ})$.

Remarks

1. Each complete execution of Steps 1–3 is referred to as a *try*. Among all tries that

achieve $S = 0$, the CBBD algorithm selects the best design using a lexicographic ordering of f in Step 3: it first maximizes the determinant-based efficiency d_2, and then minimizes the correlation pair (r_{QQ}, r_{II}). Note that unlike OMA designs, the OMA*designs, those with $S = 0$ also satisfy $r_{QI} = 0$, where r_{QI} is the maximum absolute correlation between a QE and an IE.

In some cases, a foldover structure may be employed. The CBBD algorithm then constructs only the first half-design fraction (HDF), while the second fraction is obtained by reversing the signs of all elements in the first HDF. In this case, the construction of the HDF in Step 1 does not require the constraint that the sum of all nonzero elements of C equals zero.

2. The algorithm is computationally efficient for three reasons. First, it operates on the compact circulant matrix C of size $r \times m$ rather than the full design matrix $rm \times m$, reducing memory and computational cost. Second, candidate swaps are evaluated through incremental updates of the moment vector J, avoiding full recomputation. Third, the search terminates immediately once a configuration with $S = 0$ is found.

To assess the practical computational effort, we recorded the runtime required to generate the designs in Table 1. Each parameter setting (m, r, n_1) was evaluated using 10,000 independent tries of the CBBD algorithm on a standard desktop computer. The runtime ranged from about 6 seconds for $m = 5$ (approximately 0.6 ms per try) to about 8 minutes for the largest successful case $(m, r, n_1) = (10, 8, 5)$ (about 49 ms per try). For the most difficult settings $(11, 8, 5)$ and $(11, 8, 6)$, more than 10,000 tries were executed without finding a satisfactory design, corresponding to runtimes of roughly 15 minutes (about 90 ms per try). In practice, however, good designs often appeared much earlier in the search, frequently within the first few hundred tries. The number of iterations (i.e., exchanges and updates required to reach $S = 0$) within a try of CBBD is typically very small, ranging from about 3–6 for $m \leq 6$ and remaining below about 15 even for the

largest successful cases.

Note that the CBBD algorithm is both faster and more effective than the approach of Nguyen et al. (2021) because it does not enforce orthogonality among interaction effects. This allows the use of a shorter vector J.

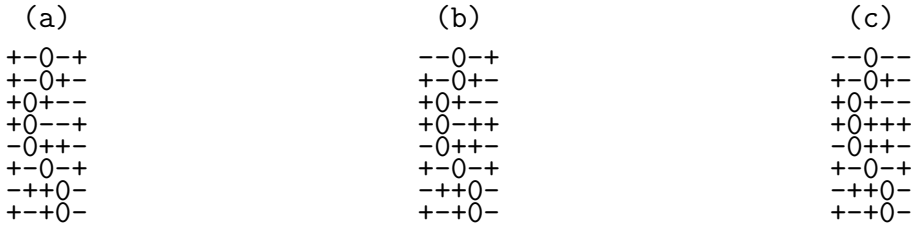

Figure 2: Steps of CBBD for constructing matrix C for the design with parameters $(m, r, n_1) = (5, 8, 4)$ shown in Figure 1.

Figure 2 illustrates the steps of the CBBD algorithm for constructing the matrix C corresponding to the design parameters $(m, r, n_1) = (5, 8, 4)$ shown in Figure 1. Figure 2(a) displays the initialization and randomization step. The moment vector J then collects the quantities appearing in the OMA* conditions (5b)–(5e). Since $m = 5$, the vector has 20 entries—4 from (5b), 4 from (5c), 6 from (5d), and 6 from (5e)—which agrees with the expression for the vector length in Eq. (6) for non-foldover designs. Readers can verify that $J =$ `(-6,-10,-10,-6,0,-2,0,2,-2,2,-2,2,2,-2,-4,-6,-8,-4,-6,-4)`, giving the initial objective value $S = \sum_j J_j^2 = 488$, for the configuration shown in Figure 2(a).

Figures 2(b)–2(c) illustrate two successive swap iterations that reduce the objective value to zero. Figure 2(b), obtained by swapping the elements C_{00} and C_{33} in Figure 2(a), produces $J =$ `(-6,-6,-6,-6,0,0,-2,2,2,-2,2,-2,-2,2,-2,-4,-4,-4,-4,-6)`, which reduces S to 280. The next swap between C_{04} and C_{32} in Figure 2(b) results in Figure 2(c), yielding the null vector J and the optimal value $S = 0$.

4 Results and Discussion

4.1 New designs

Table 1 provides a comprehensive summary of 15 CBBDs for up to 11 factors, including both exact BBDs and near-BBDs. For each design, the table reports the number of factors m, number of ± 1 levels per row, D-efficiencies d_1 and d_2 (see Equation 7), maximum absolute correlation coefficients among quadratic terms r_{QQ}, and among interaction terms r_{II}. Generating vectors used to construct the designs are also listed, serving as concise descriptors of their structure. Designs with $r_{II} = 0$ are exact BBDs, which offer ideal orthogonality between IEs, making them statistically clean and easy to interpret. Those that only meet the OMA* property but with $r_{II} > 0$ are classified as near-BBDs. Near-BBDs preserve most of the structural and orthogonality benefits of BBDs while allowing moderate aliasing among interaction effects in exchange for substantially reduced run sizes. In practice, the observed levels of aliasing (e.g., $r_{II} = 0.577$ for the 11-factor design) remain within ranges commonly considered acceptable for screening and exploratory response-surface studies.

BBDs are widely used for experiments with 3 to 7 factors because they enable full estimation of second-order models with relatively few runs—often fewer than 60—making them practical and cost-effective for industrial and scientific applications. However, as the number of factors exceeds 7, traditional BBDs require substantially more runs (often over 100), limiting their feasibility in time- or budget-constrained studies.

The six new near-BBDs for 8 to 11 factors in Table 1 address this limitation. They achieve run sizes well below 100 while maintaining high D-efficiency and acceptable aliasing, offering a practical option for efficient second-order modeling in high-dimensional settings where traditional BBDs are unavailable or excessively large. These designs fill a critical gap in the literature and represent a valuable resource for researchers. Notably,

Table 1: Design properties of BBDs and near-BBDs and generating vectors with up to 11 factors and fewer than 100 runs†

m	n_1	d_1	d_2	r_{QQ}	r_{II}	Generating vectors
5‡	2	0.302	0.174	0.212	0	0+0+0;000++;00−−0;0−0−0; +00−0;00+0−;00+−0;0−+00
5‡	3	0.338	0.303	0.556	0	0−+−0;−+00+;00−−−;++00−; 0−−+0;00+++;00+−−;−00++
5‡	4	0.406	0.429	0.050	0.333	−−0−−;+−0+−;+0+−−;+0+++; −0++−;+−0−+;−++0−;+−+0−
6‡	3	0.335	0.243	0.359	0	−0−00+;+0+00+;−00−−0;0+−0+0; +0−00−;00++0−;00−−0+;0+00−+
6	5	0.387	0.484	0	0.250	+−0−+−;−+0+++;+−−−0+;+0+−−+; −−+0−−; +0−+++;0−−+−−;++−0+−
7‡	3	0.321	0.196	0.137	0	0−0−−00;0+0−+00;00+0−−0;++000+0; −000−0+;−0++000;0−0−+00;000+0+−
7‡	4	0.381	0.276	0.115	0.500	0+0−−+0;−0++−00;00+0+++;−0−−−00; 00+0+−−; −00+0−+;+00−0+−;++00−0−
7	5	0.330	0.370	0.356	0.333	−−00+−−;00++++−;−−00−+−;++00−+−; +00−−+−;−++00+−;00−−++−;+00+++−
7	6	0.368	0.516	0.033	0.200	+−+0+++;++−0++−;+−−−0−+;−−+0+−−; 0+−+−+−;−++++0−;−−0−−−+;0−+−−++
8	5	0.373	0.325	0.523	0.408	−0+−−+00;0+0−−++0;0+0−−−−0;00−0−+++; −−00−0−+;−00+0+++;+−00−0+−;−+00+0++
9	5	0.348	0.262	0.306	0.408	00−0−0−+−;00+0+0++−;0−0+0−−−0;++00+0+0−; −−+00+0−0;00−0+0+−+;0+0−0+−−0;+00−0−0++
9	6	0.357	0.333	0.423	0.289	−00+0−−++;0+−−++00+;−−−−00−0+;++−+00+0+; −00−0++++;00+0−+−−−;00−0−−+−+;0−0−+−++0
10	5	0.336	0.214	0.219	0.500	0−0−−0−+00;0+0+−0+−00;−−000−0++0;0++000+0−+; −−000+0−+0;00−0++0++0;+−000−0−−0;−0−+000+0+
11	5	0.273	0.159	0.440	0.577	0000−−+00−−;0000+−+00+−;000−+−00+−0;00++0000+−−; 000−−−00−+0;−++00++0000;+−00−−0000+;000+++00−+0
11	6	0.303	0.224	0.429	0.408	0−0−−−+000−;+000−0+0+−+;000−0+0−++−;+++000+0−0+; 0−0++−−000−;−−+−000+0−0;00+0+0+−−−0;−+000+0+0−+

† The number of runs of each design is $n = 8m + 2$.

‡ Foldover solution available.

Nguyen et al. (2021) were unable to identify designs for 8–11 factors that meets the OMA or OMA* conditions using fewer than 100 runs.

4.2 An example of using near-BBD

Let us revisit the 8-factor BBD used in Gan, Fang and Wei (2021), as mentioned in the Introduction. Although this design does not originate from Box and Behnken (1960), it follows the same core principle: all possible $\binom{8}{2} = 28$ factor pairs define incomplete blocks. Each block generates four runs by varying the selected pair while holding the

remaining six factors at level 0, resulting in $28 \times 4 = 112$ factorial runs, plus eight center points. For instance, the first four runs are $(\pm 1, \pm 1, 0, 0, 0, 0, 0, 0)$ (see Table 5 in Gan, Fang and Wei (2021)).

A proposed alternative is a near-BBD for eight factors with 64 runs plus two center points, shown in Table 1 and visualized in Figure 3. The goodness measures $(d_1, d_2, r_{\mathrm{QQ}}, r_{\mathrm{QI}}, r_{\mathrm{II}})$ for the 8-factor BBD with eight center points are $(0.274,\ 0.067,\ 0.118,\ 0,\ 0)$, while the corresponding values for the proposed design are $(0.373,\ 0.325,\ 0.523,\ 0,\ 0.408)$.

-0+--+00	0+0--++0	0+0----0	00-0-+++	--00-0-+	-00+0+++	+-00-0+-	-+00+0++
0-0+--+0	00+0--++	00+0----	+00-0-++	+--00-0-	+-00+0++	-+-00-0+	+-+00+0+
00-0+--+	+00+0--+	-00+0---	++00-0-+	-+--00-0	++-00+0+	+-+-00-0	++-+00+0
+00-0+--	++00+0--	--00+0--	+++00-0-	0-+--00-	+++-00+0	0+-+-00-	0++-+00+
-+00-0+-	-++00+0-	---00+0-	-+++00-0	-0-+--00	0+++-00+	-0+-+-00	+0++-+00
--+00-0+	--++00+0	----00+0	0-+++00-	0-0-+--0	+0+++-00	0-0+-+-0	0+0++-+0
+--+00-0	0--++00+	0----00+	-0-+++00	00-0-+--	0+0+++-0	00-0+-+-	00+0++-+
0+--+00-	+0--++00	+0----00	0-0-+++0	-00-0-+-	00+0+++-	-00-0+-+	+00+0++-

Figure 3: 64 non-center rows of a near-BBD for eight factors.

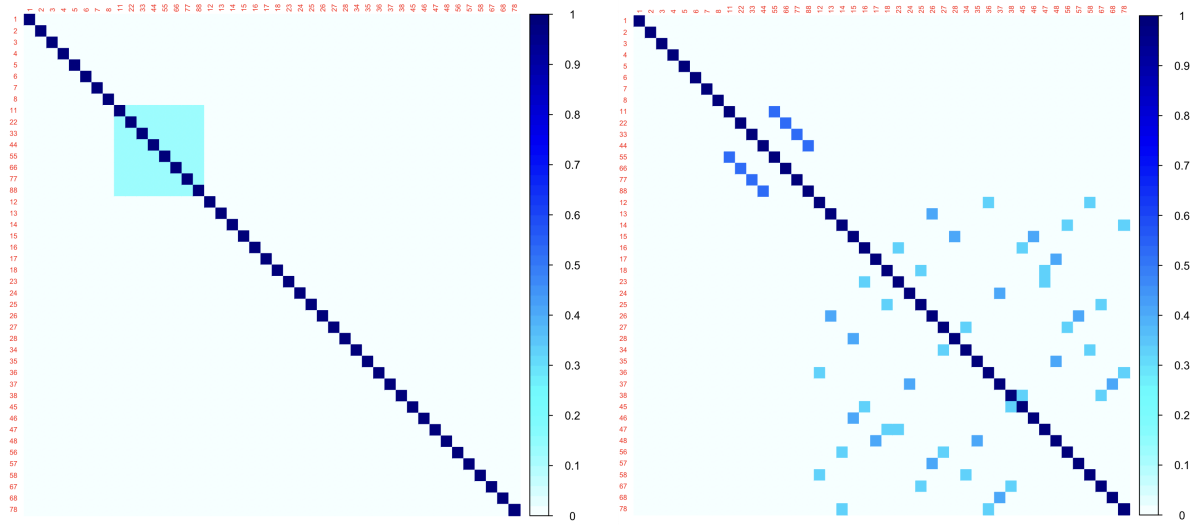

(a) (b)

Figure 4: CCPs of (a) a BBD for eight factors; and of (b) a near-BBD for eight factors.

The D-efficiency values reported here should not be interpreted as a direct ranking between designs with different run sizes (see Goos, 2009). Rather, they serve as descriptive indicators of how effectively each design spreads information across the second-order

model. In the present case, the relatively low d_2 value of the BBD reflects the sparse structure of the design: each run changes only two factors while the remaining six are fixed at 0. Consequently, the design points occupy only a small subset of the eight-dimensional design space, leading to less efficient use of experimental runs.

Color correlation plots (CCPs; see Jones and Nachtsheim (2011)) comparing the two designs are shown in Figure 4.

4.3 CBBD algorithm and OMARS designs

Núñez Ares and Goos (2020) introduced a new family of orthogonal minimally aliased response surface (OMARS) designs. These designs are constructed to ensure that MEs are unaliased with SOEs, including both QEs and IEs. Figure 5 (a) presents an example of a 7-factor OMARS design (Design # 3 from Ares and Goos, 2020, p. 29). In comparison, Figure 5 (b) shows an alternative design generated using the proposed CBBD approach for the same 7-factor setting where the OMA criterion was applied. Both designs have identical numbers of ± 1 and 0 entries.

(a)

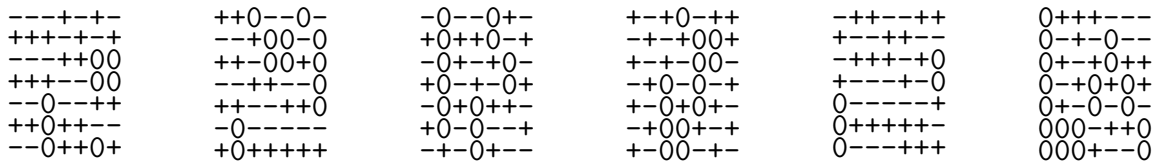

(b)

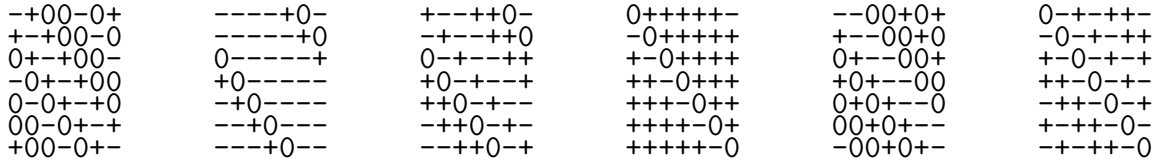

Figure 5: Two OMARS designs for seven factors: (a) Design 3 of Núñez Ares and Goos, 2020, p. 29); (b) An alternative design constructed by the CBBD algorithm.

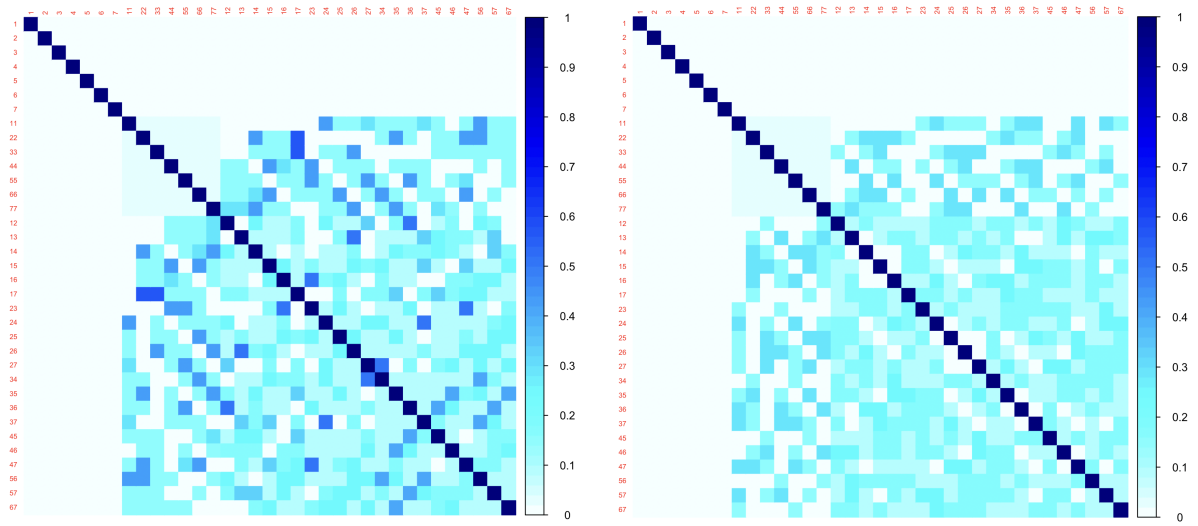

(a) (b)

Figure 6: CCPs of (a) an OMARS design for seven factors; and (b) an alternative design for seven factors.

The goodness measures $(d_1, d_2, r_{\mathrm{QQ}}, r_{\mathrm{QI}}, r_{\mathrm{II}})$ for the OMARS design (with one center run) are (0.772, 0, 0.023, 0.571, 0.5), while those for the alternative design (with one center run) are (0.772, 0.332, 0.023, 0.285, 0.25), indicating improved D-efficiency and orthogonality between QEs and IEs in the alternative design. Comparative CCPs for the two designs are shown in Figure 6. Notably, among the OMARS designs with 5 to 7 factors, only the 7-factor design could be improved. This observation suggests that the CBBD algorithm may provide more effective design constructions than the integer programming approach of Núñez Ares and Goos (2020) for larger factor settings.

5 Blocking BBDs and near-BBDs

When an experiment requires a large number of runs, blocking becomes essential to mitigate the effects of uncontrolled sources of variability such as time trends, operator differences, or environmental changes. By distributing treatments across relatively homogeneous blocks, blocking prevents confounding between treatment effects and nuisance factors, improves the precision of effect estimation, reduces experimental error, and

enhances the reliability of experimental conclusions. In addition, partitioning a large experiment into smaller and more manageable subgroups improves logistical feasibility. General blocking strategies for OMARS-type designs, including near-BBDs, can be found in Nguyen et al. (2021) and Núñez Ares & Goos (2023).

The original Box–Behnken designs of Box and Behnken (1960) were derived from two-level factorial structures and are typically partitioned into two to six blocks using a single blocking factor. In many practical settings, however, experiments may involve multiple nuisance sources, making the use of more than one blocking factor desirable.

Session 1 LC-1	Session 1 LC-2	Session 2 LC-1	Session 2 LC-2
00+0--++	+--00-0-	-00+0---	+0+++-00
+00-0+--	--00-0-+	-00-0+-+	0-0-+++0
--++00+0	-0+--+00	+0----00	00000000
+-00+0++	0----00+	0+++-00+	-0-+--00
-0+-+-00	+--+00-0	00-0-+--	+00+0++-
0-0+-+-0	+00-0-++	++-+00+0	-++00+0-
-+-00-0+	0+0+++-0	-+00+0++	--+00-0+
0+-+-00-	+0++-+00	0--++00+	-+--00-0
-+++00-0	+00+0--+	0-0-+--0	0-+++00-
00000000	-00+0+++	0-0+--+0	+-00-0+-
+++00-0-	0+0++-+0	-0-+++00	+++-00+0
+0--++00	0++-+00+	0+0--++0	++00+0--
--00+0--	---00+0-	+-+00+0+	00+0++-+
00-0+-+-	0+--+00-	++-00+0+	00000000
+-+-00-0	00-0-+++	++00-0-+	00-0+--+
00000000	-+00-0+-	-00-0-+-	----00+0
00+0+++-	0+0----0	0-+--00-	00+0----

(a)

Session 1 LC-1	Session 1 LC-2	Session 2 LC-1	Session 2 LC-2	Session 3 LC-1	Session 3 LC-2
00-0+--+	0+0++-+0	-+-00-0+	0-0-+--0	00+0----	0-0+--+0
00+0+++-	-00+0---	---00+0-	-0+-+-00	00+0--++	-++00+0-
-+--00-0	00+0++-+	00-0-+++	+00-0+--	+++-00+0	+0----00
-+00-0+-	0-0-+++0	0+0----0	+0++-+00	0--++00+	0+-+-00-
++-00+0+	+-00+0++	+0+++-00	-00+0+++	--00-0-+	0----00+
0-+++00-	+00-0-++	-00-0-+-	00000000	+-+00+0+	+++00-0-
-0+--+00	++00-0-+	0-0+-+-0	0+0--++0	0++-+00+	-0-+++00
0+--+00-	0-+--00-	+-+-00-0	+00+0--+	++00+0--	-00-0+-+
00-0-+--	+-00-0+-	00000000	+0--++00	-+00+0++	----00+0
--+00-0+	0+++-00+	++-+00+0	00-0+-+-	+--00-0-	--00+0--
+--+00-0	-0-+--00	--++00+0	-+++00-0	+00+0++-	0+0+++-0

(b)

Figure 7: The near-BBD for eight factors in Figure 6, blocked using two factors (i) test sessions and distinct landing conditions (LC-1: regular and LC-2: extreme): (a) two sessions (four center runs) ; (b) three sessions (two center runs).

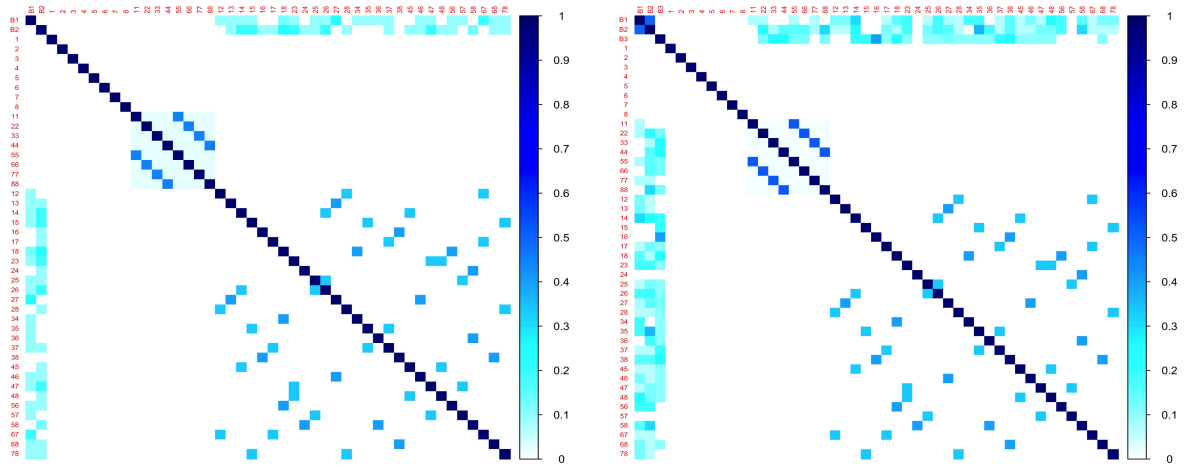

(a) (b)

Figure 8: CCPs show the alias structure between the blocking factors and the MEs and SOEs of (a) the blocked design in Figure 7 (a) and (b) the blocked design in Figure 7 (b).

Returning to the motivating example described in the Introduction, improving the operational feasibility and robustness of the proposed design requires incorporating two blocking factors. First, because the experiment is conducted over multiple periods, introducing blocks corresponding to two or three test sessions per day helps account for potential nuisance variation arising from equipment drift, operator fatigue, and changes in ambient conditions. Second, the experiment involves two distinct landing conditions (LC-1: regular and LC-2: extreme). Treating landing condition as a blocking factor controls for systematic differences in landing dynamics and energy absorption. Incorporating these two blocking factors isolates nuisance variability that is not of primary interest and enables more accurate estimation of the model effects.

Figures 7(a) and 7(b) illustrate the eight-factor near-BBD (see Figure 3) blocked according to the two factors described above. Figure 7(a) corresponds to blocking by two sessions and landing conditions (with four center runs), whereas Figure 7(b) corresponds to three sessions and landing conditions (with two center runs).

Figures 8(a) and 8(b) present the color correlation plots (CCPs) illustrating the alias structure between the blocking factors and the MEs and second-order effects (SOEs). In

Figure 8(a), the two blocking factors are orthogonal to the MEs and QEs and only mildly aliased with the IEs; the maximum absolute correlation between block effects (using effect coding) and IEs is 0.243. In Figure 8(b), the blocking factors remain orthogonal to the MEs but exhibit slight aliasing with certain SOEs. The maximum absolute correlation between block effects (using effect coding) and QEs is 0.304 and with IEs is 0.402. These CCPs confirm that the proposed blocking schemes preserve the primary orthogonality structure of the design while introducing only limited confounding with higher-order effects.

6 Conclusion

This paper introduces a new class of three-level, second-order response surface designs, termed Circulant Matrix-Based Box–Behnken Designs (CBBDs), that overcome scalability limitations of traditional BIBD and partially BIBD-based BBD constructions.

Traditional BBDs already possess two important orthogonality properties: (i) the OMA* property, under which MEs are mutually orthogonal and orthogonal to all SOEs, while QEs are orthogonal to IEs; and (ii) mutual orthogonality among the IEs. However, when constructed from incomplete block designs (IBDs), such designs often require large numbers of runs, particularly as the number of factors increases.

The proposed CBBD framework exploits circulant matrix structures to generate BBDs and near-BBDs that retain most of the essential geometric and statistical characteristics of classical BBDs—including the OMA* property—while substantially reducing the number of runs. Cyclic symmetry in the generating vectors enables compact representation and computationally efficient construction, yielding high D-efficiency and improved design economy without sacrificing key orthogonality properties.

In summary, CBBDs provide a scalable, computationally efficient, and statistically robust alternative to traditional IBD-based BBDs. By combining circulant structure

with the intrinsic OMA* property of BBDs, CBBDs allow efficient exploration of complex response surfaces with fewer runs, minimal aliasing, and strong theoretical guarantees, making them well suited for modern industrial and scientific experimentation.

Acknowledgement

We are grateful to the reviewers for their careful reading and constructive comments. Their insightful suggestions have helped improve the clarity, presentation, and overall quality of the paper, making the manuscript more readable.

Data Availability

The data that supports the findings of this study are available in the supplementary material of this article.

Disclosure of interest

We have no conflicts of interest to disclose.

Declaration of funding

No funding was received.

References

[1] Box, G. E. P., & Behnken, D. (1960). Some new three level designs for the study of quantitative variables. *Technometrics*, *2*(4), 455–475.

[2] Gan, S., Fang, X., & Wei, X. (2021). Parametric analysis on landing gear strut friction of light aircraft for touchdown performance. *Applied Sciences*, *11*(12), 5445. https://doi.org/10.3390/app11125445

[3] Georgiou, S. D., Stylianou, S., & Aggarwal, M. (2014). Efficient three-level screening designs using weighing matrices. *Statistics*, *48*, 815–833.

[4] Goos, P. (2009). Discussion of "Response surface design evaluation and comparison". *Journal of Statistical Planning and Inference*, *139*(2), 657–659.

[5] Jones, B., & Nachtsheim, C. J. (2011). A class of three-level designs for definitive screening in the presence of second-order effects. *Journal of Quality Technology*, *43*(1), 1–15. https://doi.org/10.1080/00224065.2011.11917841

[6] Jones, B., & Nachtsheim, C. J. (2011). Efficient designs with minimal aliasing. *Technometrics*, *53*, 62–71. https://doi.org/10.1198/TECH.2010.09113

[7] Nguyen, N. K., & Borkowski, J. J. (2008). New 3-level response surface designs constructed from incomplete block designs. *Journal of Statistical Planning and Inference*, *138*, 294–305.

[8] Nguyen, N. K., Pham, T. D., & Vuong, P. M.,(2021). Multiway Blocking of Designs of Experiments. *Statistics and Applications 19*(1), 247–255.

[9] Nguyen, N. K., Stylianou, S., Pham, T. D., & Vuong, M. P. (2026). Constructing orthogonal minimally aliased response surface designs using circulant weighing matrices. *Journal of Quality Technology*, *58*(1), 24–35. https://doi.org/10.1080/00224065.2025.2581890

[10] Núñez Ares, J., & Goos, P. (2020). Enumeration and multicriteria selection of orthogonal minimally aliased response surface designs. *Technometrics*, *62*, 21–36.

[11] Núñez Ares, J., & Goos, P. (2023), Blocking OMARS Designs and Definitive Screening Designs. *Journal of Quality Technology*, *55*, 489–509.

[12] Pham, T. D., Nguyen, N. K., Tran, M. C., & Vuong, P. M. (2020). Constructing response surface designs with orthogonal quadratic effects using cyclic generators. *Chemometrics and Intelligent Laboratory Systems*, *198*, 103918. https://doi.org/10.1016/j.chemolab.2019.103918